

The η' meson at the physical point with $N_f = 2$ Wilson twisted mass fermions

Christopher Helmes¹, Bastian Knippschild¹, Bartosz Kostrzewa¹, Liuming Liu¹, Christian Jost¹, Konstantin Ottnad^{1,2}, Carsten Urbach^{1,*}, Urs Wenger³, and Markus Werner¹
for the ETM collaboration

¹HISKP (Theory) and Bethe Center for Theoretical Physics, University of Bonn, Germany

²Institut für Kernphysik, Johannes Gutenberg-Universität Mainz, Germany

³ITP, Albert Einstein Center for Fundamental Physics, University of Bern, Switzerland

Abstract. We present results for the η' meson and the topological susceptibility in $N_f = 2$ flavour lattice QCD. The results are obtained using Wilson twisted mass fermions at maximal twist with pion masses ranging from 340 MeV down to the physical point. A comparison to literature values is performed giving a handle on discretisation effects.

1 Introduction

Due to the persisting $3 - 5 \sigma$ deviation in the anomalous magnetic moment of the muon a_μ between theory and experiment there is considerable interest in the decays $\eta \rightarrow \gamma^* \gamma^*$ and $\eta' \rightarrow \gamma^* \gamma^*$. A better knowledge of the corresponding transition form factors could help to reduce the uncertainty in the hadronic light-by-light contribution to a_μ , see for instance Ref. [1]. Moreover, η and η' mesons are interesting from a theoretical point of view because the large mass of the η' meson is explained by the anomalously broken $U_A(1)$ axial symmetry in QCD. The η, η' mixing pattern and the aforementioned transition form factors can be computed non-perturbatively using lattice techniques. There has been considerable progress in studying η and η' mesons from lattice QCD. In Ref. [2] the corresponding mixing has been studied for three values of the lattice spacing and a large, but still unphysical range of pion mass values in $N_f = 2 + 1 + 1$ flavour QCD. After extrapolation to the physical pion mass value excellent agreement to experiment was found. Further lattice results for η, η' can be found in Refs. [3–6], however, all at a single lattice spacing value and unphysically large pion mass values. In Refs. [7, 8] the continuum limit has been studied.

In this proceeding we attempt to study the η' meson directly at the physical point, in a first step in $N_f = 2$ flavour QCD. In $N_f = 2$ flavour QCD there exists a pion triplet and one flavour singlet, which is related to the aforementioned anomaly. We will denote it as η_2 meson to distinguish it from the η' meson in full QCD, which is only approximately a flavour eigenstate. The η_2 and the η' meson have in common that both receive significant fermionic disconnected contributions to their correlation functions. Their masses are expected to differ only by 200 MeV, since the strange quark is expected to contribute significantly less than the light quarks [9]. In particular, both are expected to have a similar

*Speaker, e-mail: urbach@hiskp.uni-bonn.de

Table 1. The gauge ensembles used in this study. The labelling of the ensembles follows the notations in Ref. [13]. In addition to the relevant input parameters we give the lattice volume $(L/a)^3 \times T/a$ and the number of evaluated configurations N_{conf} .

| ensemble | β | c_{sw} | $a\mu_\ell$ | $(L/a)^3 \times T/a$ | $N_{\text{conf}}^{\eta_2}$ | $N_{\text{conf}}^{\chi_r}$ |
|------------------|---------|-----------------|-------------|----------------------|----------------------------|----------------------------|
| <i>cA2.09.48</i> | 2.10 | 1.57551 | 0.009 | $48^3 \times 96$ | 615 | 1277 |
| <i>cA2.30.48</i> | 2.10 | 1.57551 | 0.030 | $48^3 \times 96$ | 352 | 702 |
| <i>cA2.30.24</i> | 2.10 | 1.57551 | 0.030 | $24^3 \times 48$ | – | 703 |
| <i>cA2.60.32</i> | 2.10 | 1.57551 | 0.060 | $32^3 \times 64$ | 337 | 2590 |
| <i>cA2.60.24</i> | 2.10 | 1.57551 | 0.060 | $24^3 \times 48$ | – | 1611 |

dependence on the light quark mass. The most recent lattice QCD study of the η_2 meson can be found in Ref. [10].

Hence, studying the η_2 meson at the physical point will reveal on the one hand important qualitative information on the realisation of the anomaly in QCD. On the other hand it represents a feasibility study for a later investigation of η and η' in $N_f = 2 + 1 + 1$ QCD at the physical point [11]. The results obtained here are also important prerequisites for an exploratory study of $\eta_2 \rightarrow \gamma^* \gamma^*$.

Since the η_2 meson is tightly connected to topology, we augment this study by measuring the topological susceptibility as well. For this purpose we apply gradient flow techniques [12] and compare to results available in the literature.

2 Lattice Action and Operators

The results presented in this paper are based on the gauge configurations generated by the ETMC with Wilson clover twisted mass quark action at maximal twist [14]. We employ the Iwasaki gauge action [15]. The measurements are performed on up to five $N_f = 2$ ensembles with pion mass at its physical value, 240 MeV and 340 MeV, respectively. The lattice spacing is $a = 0.0931(2)$ fm for all three ensembles. In Table 1 we list the five ensembles with the relevant input parameters, the lattice volume and the number of configurations. More details about the ensembles can be found in Ref. [13].

As a smearing scheme we use the stochastic Laplacian Heaviside (sLapH) method [16, 17] for our computation. The details of the sLapH parameter choices for a set of $N_f = 2 + 1 + 1$ Wilson twisted mass ensembles are given in Ref. [18]. The parameters for the ensembles used in this work are the same as those for $N_f = 2 + 1 + 1$ ensembles with the corresponding lattice volume.

In $N_f = 2$ flavour QCD there is the neutral pion, corresponding to the neutral one of the three pions in the triplet, and the η_2 , the flavour singlet pseudo-scalar meson related to the axial $U(1)$ anomaly. The (hermitian) interpolating operator projected to zero momentum reads

$$O^s(t) = \frac{1}{\sqrt{2}} \sum_{\mathbf{x}} \bar{\psi}(\mathbf{x}, t) i\gamma_5 \mathbb{1}_f \psi(\mathbf{x}, t). \quad (1)$$

Here, $\mathbb{1}_f$ is the unit matrix acting in flavour space. From the operator one builds the correlation functions

$$C_{\eta_2}(t - t') = \langle O^s(t) (O^s(t'))^\dagger \rangle, \quad (2)$$

which allows one to determine the mass M_{η_2} from its decay in Euclidean time.

The correlation function in Eq. 2 has both a fermionic connected and a fermionic disconnected contribution. The connected contribution can be estimated with high statistical accuracy. It decays

asymptotically exponentially with the mass of the (connected neutral) pion. The disconnected part is statistically noisy. The signal for the η_2 meson arises from the difference of connected and disconnected contribution,

$$C_{\eta_2}(t) = C^{\text{conn}}(t) - C^{\text{disc}}, \quad (3)$$

where the disconnected contribution has to cancel the pion contribution coming from the connected part. Since the pion is significantly lighter than the η_2 , the statistical analysis is rather delicate.

The topological susceptibility is a measure for the fluctuations of the topological charge. It is defined as

$$\chi_t = \frac{1}{V} \int dx \int dy \langle q(x)q(y) \rangle \quad (4)$$

with the volume V and the topological charge density $q(x)$ for which we use a clover-type discretisation of the field strength tensor, following the conventions in Ref. [19]. For the topological susceptibility χ_t we employ the gradient flow as introduced for lattice QCD in Ref. [12]. This setup has the advantage of yielding a renormalised topological susceptibility at any finite flow time t . Since the renormalised susceptibility is scale invariant, it becomes independent of t at sufficiently large flow times. This is indeed what we observe in our calculation and we choose $t = 3t_0$ with $\sqrt{t_0} = 0.1535(12)$ fm from Ref. [13] obtained at the physical point.

3 Analysis

The data is analysed using a blocked bootstrap procedure with $R = 1500$ bootstrap samples. Depending on the ensemble, we have chosen the block size such that roughly 150 blocked data points were left. For the analysis of the topological susceptibility we use $R = 1000$ bootstrap samples and block sizes yielding around 100 data blocks depending on the ensemble under consideration. The resulting error is compared to the naive one appropriately rescaled with the integrated autocorrelation time of Q^2 , and the larger of the two is chosen as the final error.

3.1 Excited State Subtraction

In particular for the η_2 meson, the fermionic disconnected contributions are very noisy. As a consequence, the signal is lost relatively early in Euclidean time. For this reason we have in the past applied a method to subtract excited states [2, 10, 20], originally proposed in Ref. [21]. Because it works very well, we will apply it here again for the η_2 meson. It consists of subtracting excited states from the connected contribution only. This is feasible, because the connected part – representing a pion correlation function – has a signal for all Euclidean time values. Therefore, we can fit it at large enough Euclidean times such that excited states have decayed sufficiently. Next, we replace the connected correlation function at small times by the fitted function. Thereafter, the such subtracted connected contribution is summed according to Eq. 3 to the full η_2 correlation functions.

The underlying assumption is that disconnected contributions are large for the ground state, i.e. the η_2 , but not for excited states. If this assumption is correct, the effective mass

$$M_{\text{eff}} = -\log \frac{C_{\eta_2}(t)}{C_{\eta_2}(t+1)} \quad (5)$$

should show a plateau from very early Euclidean times on. We have found in Refs. [2, 10] that this approach works very well for the η_2 meson in $N_f = 2$ flavour QCD as well as for η and η' mesons in $N_f = 2 + 1 + 1$ flavour QCD.

Phenomenologically, the connected contribution gives the pion as the ground state for large Euclidean times. And, due to symmetries, it cannot couple to the η_2 . The pion contribution needs to be cancelled by the disconnected contribution, which, therefore, reads

$$C_{\eta_2}^{\text{disc}} \approx A \cdot e^{-M_{\pi^0} t} - B \cdot e^{-M_{\eta_2} t}$$

if no higher excited states contribute.

3.2 Shifted Correlation Functions

The expected time dependence of the correlation functions considered here reads as follows

$$C(t) = |\langle 0 | \mathcal{O}^s | 0 \rangle|^2 + \sum_n \frac{|\langle 0 | \mathcal{O}^s | n \rangle|^2}{2E_n} (e^{-E_n t} + e^{-E_n(T-t)}), \quad (6)$$

where n labels the states with the corresponding quantum numbers. The first, time independent term on the right hand side corresponds to the vacuum expectation value (vev). Using the symmetries of our action one can show that for \mathcal{O}^s the vev must be zero. Potential deviations from this expectation due to finite statistics and volume can be dealt with by building the shifted correlation function

$$\tilde{C}(t) = C(t) - C(t+1). \quad (7)$$

The difference cancels any constant contributions in the correlation function, while also changing the time dependence to be anti-symmetric in time

$$\tilde{C}(t) \propto (e^{-E_n t} - e^{-E_n(T-t)}). \quad (8)$$

In addition, there can be finite volume effects due to incorrectly sampled topological charge sectors. The corresponding formulae for fixed topological sectors have been worked out in Ref. [22]. They lead to a finite volume effect in C_{η_2} constant in Euclidean time of the form [23]

$$\propto \frac{a^5}{T} \left(\chi_t - \frac{Q^2}{V} \right) \quad (9)$$

proportional to the difference of the topological susceptibility, χ_t , and the expectation value of the squared topological charge Q^2/V . If present, such a term will cause the η_2 correlation function to stay finite at large Euclidean times. Depending on the sign of the coefficient in front of the finite volume effect, the correlation function may even turn negative at relatively small Euclidean times. Clearly, a finite volume effect of this type can be subtracted again using the shifting procedure.

The shifting procedure has the additional advantage of removing statistical correlations between neighbouring time slices t/a and $t/a + 1$. Therefore, shifting can also be advantageous for the analysis procedure, because the inverse variance-covariance matrix is often difficult to estimate reliably [24]. Of course, when the correlation between adjacent time slices can be taken into account correctly, there is no difference in using the unshifted or the shifted correlation function and both give exactly identical results (unless there is a constant contribution).

3.3 Scale Setting

In order to compare the η_2 masses to older publications available in the literature, we use the Sommer scale r_0/a for the M_{η_2} . The value $r_0/a = 5.317(48)$ from Ref. [13] for the *cA2.09.48* ensemble at

the physical point is used for all ensembles considered here. The corresponding physical value reads $r_0 = 0.4907(5)$ fm.

Since we use the gradient flow to determine the topological susceptibility, it is natural to use a scale from the gradient flow for χ_t . In order to compare our results with the ones from Ref. [19] we use the scale $t_1(m_\pi)$. Its physical value at the physical point reads $t_1 = 0.061$ fm² [19]. Note, however, that χ_t is evaluated at flow time $t = 3t_0$ as discussed above.

4 Results

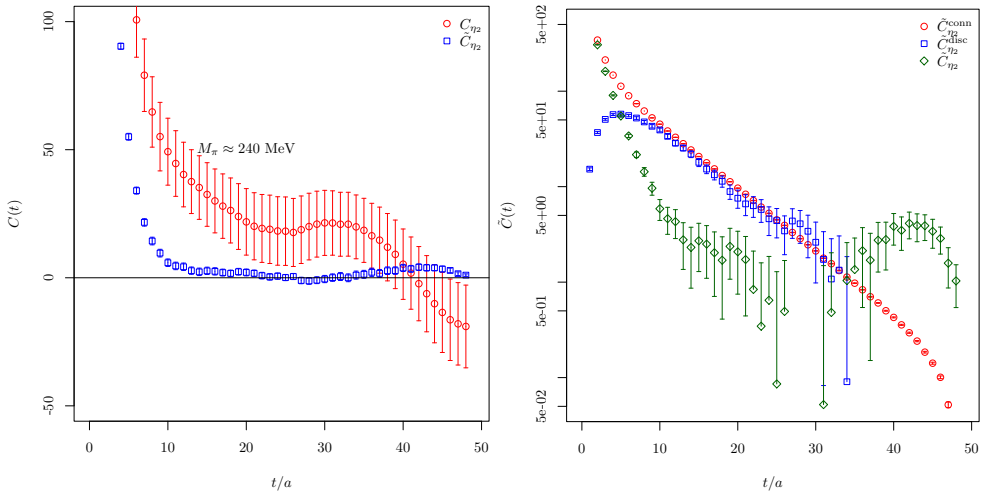


Figure 1. Left: η_2 correlation function C_{η_2} and its shifted counterpart \tilde{C}_{η_2} for ensemble cA2.30.48 as a function of t/a . Right: connected, disconnected and full shifted correlation function \tilde{C}_{η_2} as a function of t/a with logarithmic y -axis.

In the left panel of Figure 1 we show the η_2 correlation function C_{η_2} and the corresponding shifted one \tilde{C}_{η_2} as functions of the Euclidean time for ensemble cA2.30.48. For C_{η_2} errors are larger than the typical fluctuations for $t/a > 10$, pointing towards large correlation between separate time slices. Still, the correlation function is not incompatible with zero at large times. In the shifted correlation function \tilde{C}_{η_2} the correlation is largely removed and the error bars are of the typical fluctuation size. Also \tilde{C}_{η_2} is compatible with zero for large times $t/a > 15$.

In the right panel of Figure 1 we show the different contributions to the η_2 shifted correlation function for ensemble cA2.30.48 in a logarithmic plot. While the signal for the connected part (red circles) is excellent up to $t/a = 48$, the disconnected contribution (blue squares) starts to become noisy around $t/a = 15$. We observe that connected and disconnected contributions are very similar in magnitude from around $t/a = 10$ on. The full η_2 correlator (green diamonds) is given by the difference of connected and disconnected parts. Consequently, the signal deteriorates around $t/a = 10$.

From the left panel of Figure 1 it is also clear that the ground state energy and amplitude of the connected contribution (in twisted mass the connected neutral pion) can be extracted reliably. The connected contribution is then replaced by only this ground state and the full disconnected part is subtracted from it. As a result we obtain plateaus from $t/a = 3$ on.

Table 2. Results for the η_2 meson in lattice units and for the topological susceptibility in units of t_1^2 for the ensembles investigated here.

| Ensemble | aM_{η_2} | $10^3 t_1^2 \chi_t$ |
|-----------|---------------|---------------------|
| cA2.09.48 | 0.358(9) | 0.53(4) |
| cA2.30.48 | 0.372(8) | 0.63(6) |
| cA2.30.24 | — | 0.52(6) |
| cA2.60.32 | 0.374(7) | 0.91(5) |
| cA2.60.24 | — | 0.91(8) |

The such extracted energy levels in lattice units are compiled in Table 2. The η_2 masses are shown in units of the Sommer parameter r_0 in Figure 2 as a function of the squared pion mass $(r_0 M_{\pi^\pm})^2$. The red circles represent the results presented here. In addition we show results for Wilson twisted mass fermions with $N_f = 2$ dynamical quark flavours without clover term taken from Ref. [10]. The blue squares correspond to a lattice spacing of about 0.09 fm, while the green diamonds correspond to about 0.08 fm. These results from Ref. [10] have larger statistical errors and the smallest pion mass corresponds to about 300 MeV. However, the agreement with the results presented here is good. In particular, the almost constant extrapolation to the physical point is confirmed. An estimate of lattice artefacts is difficult, but they seem to be not larger than our statistical uncertainties.

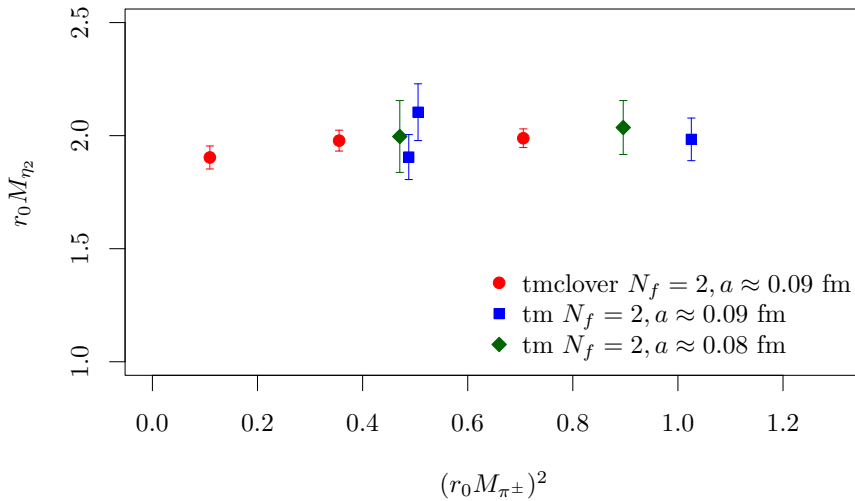


Figure 2. Compilation of $N_f = 2$ Wilson twisted mass results with and without clover term for the η_2 meson. The twisted mass (tm) results have been taken from Ref. [10].

In Table 2 we have also compiled our results for the topological susceptibility in units of t_1 . They are displayed in Figure 3 as a function of $t_1 M_{\pi^\pm}^2$. In leading order Wilson ChPT one expects the following dependence of χ_t on the lattice spacing and the pion mass [19]

$$t_1^2 \chi_t = \frac{1}{8} t_1^2 f_\pi^2 M_{\pi^0}^2 + a^2 \frac{c_2}{t_1}. \tag{10}$$

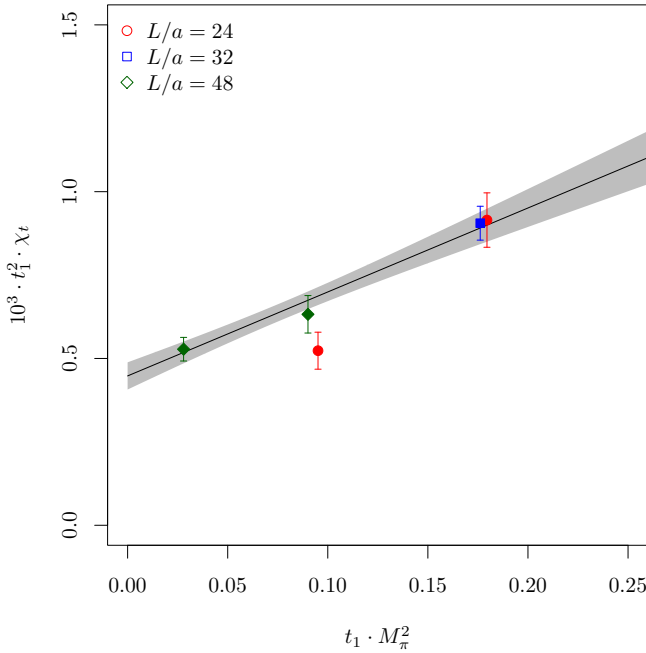


Figure 3. Topological susceptibility χ_t as a function of the squared pion mass, both in appropriate units of t_1 . The solid line with shaded error band indicates a fit to the data according to Eq. 10.

Apart from the ensemble with too small volume cA2.30.24, our data is nicely compatible with this expectation: the solid line in Figure 3 represents a fit of the function

$$g(M_{\pi^\pm}^2) = c_1 t_1 M_{\pi^\pm}^2 + a^2 \frac{c_2}{t_1}$$

to the data with fit parameters c_1 and c_2 . Note that we use the charged pion mass, because charged and neutral pion masses are degenerate within errors [13]. The best fit parameter for c_1 is compatible with $t_1 f_\pi^2/8$. Note that ensemble cA2.30.24 has a very small volume explaining the outlier in Figure 3.

The fitted value for c_2 can be compared to the results of Ref. [19]. We obtain $c_2 = 3.3(3) \cdot 10^{-3}$, while Bruno et al. have $c_2 = 5.1(7) \cdot 10^{-3}$.

5 Summary

In this proceeding contribution we have presented results for the η_2 meson related to the axial anomaly and the topological susceptibility in two-flavour QCD. The results have been obtained using $N_f = 2$ lattice QCD ensembles generated by ETMC with the Wilson twisted clover discretisation [13]. Pion mass values reach from its physical value up to 340 MeV at a single lattice spacing value of $a = 0.0931(2)$ fm. For the η_2 we could confirm the almost constant extrapolation in $M_{\pi^\pm}^2$ towards the physical point. Errors are significantly reduced compared to previous calculations. Lattice artefacts seem to be not larger than our statistical uncertainty.

The topological susceptibility has been computed using the gradient flow. As expected, χ_t is proportional to $M_{\pi^\pm}^2$ up to a lattice artefact independent of M_{π^\pm} . Even if we are not able to finally confirm this with a single lattice spacing at hand, this constant term should be of $O(a^2)$. The size of this artefact appears to be significantly smaller than what is observed with Wilson clover fermions in Ref. [19].

We thank the members of ETMC for the most enjoyable collaboration. This project was funded by the DFG as a project in the Sino-German CRC110. The computer time for this project was made available to us by the John von Neumann-Institute for Computing (NIC) on the Juqueen system in Jülich and by the ITP Bern on their HPC clusters. This work was granted access to the HPC resources of CINES and IDRIS under the allocation 52271 made by GENCI.

References

- [1] F. Jegerlehner, EPJ Web Conf. **118**, 01016 (2016), 1511.04473
- [2] C. Michael, K. Ottnad, C. Urbach (ETM), Phys.Rev.Lett. **111**, 181602 (2013), 1310.1207
- [3] N. Christ, C. Dawson, T. Izubuchi, C. Jung, Q. Liu et al., Phys.Rev.Lett. **105**, 241601 (2010), 1002.2999
- [4] J.J. Dudek, R.G. Edwards, B. Joo, M.J. Peardon, D.G. Richards et al., Phys.Rev. **D83**, 111502 (2011), 1102.4299
- [5] E.B. Gregory, A.C. Irving, C.M. Richards, C. McNeile (UKQCD), Phys.Rev. **D86**, 014504 (2012), 1112.4384
- [6] J.J. Dudek, R.G. Edwards, P. Guo, C.E. Thomas (Hadron Spectrum), Phys. Rev. **D88**, 094505 (2013), 1309.2608
- [7] H. Fukaya, S. Aoki, G. Cossu, S. Hashimoto, T. Kaneko, J. Noaki (JLQCD), Phys. Rev. **D92**, 111501 (2015), 1509.00944
- [8] S. Aoki, G. Cossu, H. Fukaya, S. Hashimoto, T. Kaneko (JLQCD) (2017), 1705.10906
- [9] C. McNeile, C. Michael (UKQCD), Phys.Lett. **B491**, 123 (2000), hep-lat/0006020
- [10] K. Jansen, C. Michael, C. Urbach (ETM), Eur.Phys.J. **C58**, 261 (2008), 0804.3871
- [11] J. Finkenrath et al. (ETM), this conference (2017)
- [12] M. Lüscher, JHEP **08**, 071 (2010), [Erratum: JHEP03,092(2014)], 1006.4518
- [13] A. Abdel-Rehim et al. (ETM) (2015), 1507.05068
- [14] R. Frezzotti, P.A. Grassi, S. Sint, P. Weisz (ALPHA), JHEP **08**, 058 (2001), hep-lat/0101001
- [15] Y. Iwasaki, Nucl. Phys. **B258**, 141 (1985)
- [16] M. Peardon, J. Bulava, J. Foley, C. Morningstar, J. Dudek, R.G. Edwards, B. Joo, H.W. Lin, D.G. Richards, K.J. Juge (Hadron Spectrum), Phys. Rev. **D80**, 054506 (2009), 0905.2160
- [17] C. Morningstar, J. Bulava, J. Foley, K.J. Juge, D. Lenkner, M. Peardon, C.H. Wong, Phys. Rev. **D83**, 114505 (2011), 1104.3870
- [18] C. Helmes, C. Jost, B. Knippschild, C. Liu, J. Liu, L. Liu, C. Urbach, M. Ueding, Z. Wang, M. Werner (ETM), JHEP **09**, 109 (2015), 1506.00408
- [19] M. Bruno, S. Schaefer, R. Sommer (ALPHA), JHEP **08**, 150 (2014), 1406.5363
- [20] L. Liu et al., Phys. Rev. **D96**, 054516 (2017), 1612.02061
- [21] H. Neff, N. Eicker, T. Lippert, J.W. Negele, K. Schilling, Phys.Rev. **D64**, 114509 (2001), hep-lat/0106016
- [22] S. Aoki, H. Fukaya, S. Hashimoto, T. Onogi, Phys. Rev. **D76**, 054508 (2007), 0707.0396
- [23] G.S. Bali, S. Collins, S. Dürr, I. Kanamori, Phys. Rev. **D91**, 014503 (2015), 1406.5449
- [24] C. Michael, A. McKerrell, Phys. Rev. **D51**, 3745 (1995), hep-lat/9412087